[AMERICAN JOURNAL OF SCIENCE, VOL. 295, SUMMER, 1995, P. 851–874]

CRUSTAL MAGMA GENERATION AND LOW-PRESSURE HIGH-TEMPERATURE REGIONAL METAMORPHISM IN AN EXTENSIONAL ENVIRONMENT; POSSIBLE APPLICATION TO THE LACHLAN BELT, AUSTRALIA

E-AN ZEN
Department of Geology,
University of Maryland,
College Park, Maryland 20742

ABSTRACT. One-dimensional thermal modelling was used to test the idea that mid-crustal anatexis of fertile sedimentary material in an extensional environment could produce abundant granitic melt. The Neogene-to-Recent crustal, tectonic, and thermal conditions of the Basin and Range Province of western United States were used to guide the modelling. The model crust was thinned from 60 to 30 km by stepwise deletion at 20 to 22, 24 to 26, or 30 to 32 km depths; the crust above the deletion depth was stationary. Near-surface crustal heat production of 2 or 3 microwatt/m^3, combined with synextensional stepwise increase of subcrustal flux from 30 to 60 or 75 milliwatt/m^2, could produce large volumes of anatectic melt above the deletion depth alone. In many model runs, the crust above the zone of melting heated isobarically through the field of stability of andalusite into that of sillimanite and even reached the second-sillimanite isograd in the absence of magma intrusion to cause coalescing contact aureoles. Results of the model are applied to the Lachlan Belt, southeastern Australia, where voluminous peraluminous, S-type granitic magma was generated by crustal anatexis during the early- to middle Paleozoic, to show that the thermal demands of magma genesis is compatible with an extensional tectonic model.

INTRODUCTION

Regional tectonic extension lasting a few tens of million years could provide the setting for large-scale magma genesis within the crust because protracted regional extension must lead to the introduction of hot, asthenospheric material to higher levels, either by underplating or by crustal intrusion. This setting is appropriate for the development of regional low-pressure, high-temperature metamorphism even in the absence of batholithic intrusions because of enhanced heat flow within the crust.

In this study, I describe a one-dimensional model of the thermal response of a large region undergoing persistent extension and enhanced heat flow to see if such regions can produce voluminous crustally-derived magma if suitable source material were available. The Basin and Range Province of western United States (B&R) provides a useful geological example because of its size, because of its high heat flow, and because detailed information on its tectonic history, amount and rate of extension, and crustal architecture are available. I then apply the results of the modelling to the problem of Silurian-Devonian magma genesis in the Lachlan Fold Belt or, following Coney (1992), the Lachlan Belt (LB), in southeastern Australia. The thermal and tectonic regimes for the production of these magmas are obscure; regional extension based on the B&R analog has been suggested by numerous workers, and my study shows that such an analogy is thermally plausible.

BASIN AND RANGE GEOLOGY: SUMMARY REVIEW

Catchings (1992) and Catchings and Mooney (1991) summarized the results of recent seismic imaging of crustal structure in the Basin and Range Province and gave references. The crustal thickness across Nevada is 30 to 35 km, having been thinned possibly by as much as 100 percent from a crust thickened during late Mesozoic orogenies (Wernicke, 1992). The upper crust, which is not penetratively deformed but is broken up by extensional, listric faults, is underlain by a zone of strong horizontal seismic reflectors. These reflectors are interpreted to be produced by ductile shear accommodating the extension. The depth of the top of this zone undulates by no more than a few kilometers (from about 15-25 km) over a distance of hundreds of kilometers.

Extensional thinning in the Nevada part of the B&R commenced during the Neogene. Wernicke and others (1988) concluded that the process has been ongoing for the last 20 my; this conclusion is supported by the distribution and dominance of normal faults active during the past 10 to 15 my (Eaton, 1980). A span of 30 my would seem a fair estimate for the extensional episode at a given place.

The amount of extensional strain depends on the location and size of the area considered and on the method of estimation. Wernicke (1992) inferred that for the central part of the province in Nevada including the Las Vegas corridor the time-averaged strain rate is about 1 to 3 $\times$ 10^{-15}/sec. It is perilous to equate the strain rate with rates of crustal thinning; however, if thinning of the crust resulted entirely in *linear* extension, that is, one of the map dimensions is held fixed where the other one changes, then halving the thickness of the crust would mean an elongation factor of 2. For 100 percent extension (=50 percent thinning) in 30 my, this means a strain rate of 1 $\times$ 10^{-15}/sec or 3 percent per my.

The regional surface heat flux for the B&R is about 80 mW/m^2 (milliwatt/square meter; 41.3 mW/m^2 = 1 microcalorie/cm^2-second; Lachenbruch and Sass, 1977, 1978; Blackwell and Steele, 1991). The flux in the area of the Battle Mountain high in northern Nevada ranges from prevailing values of 100 to 120 mW/m^2 to peak values of 160 mW/m^2. In contrast, the flux in the area of the Eureka low dips down to 40 mW/m^2 and is depressed by downward circulation of groundwater in a zone of regional recharge, carrying heat with it (Lachenbruch and Sass, 1977; Winograd and Thordarson, 1975). Lachenbruch and Sass (1977) estimated the "reduced flux," that is, the contribution to the surface flux by subcrustal heat flow where the crust has a heat-producing layer 10 km thick, to be 60 to 80 mW/m^2 (fig. 1); their extrapolation excluded data from the Eureka low that occupy the lower half of their data field. The measured heat productivity ranged from 1 to 4 uW/m^3 (microwatt/cubic

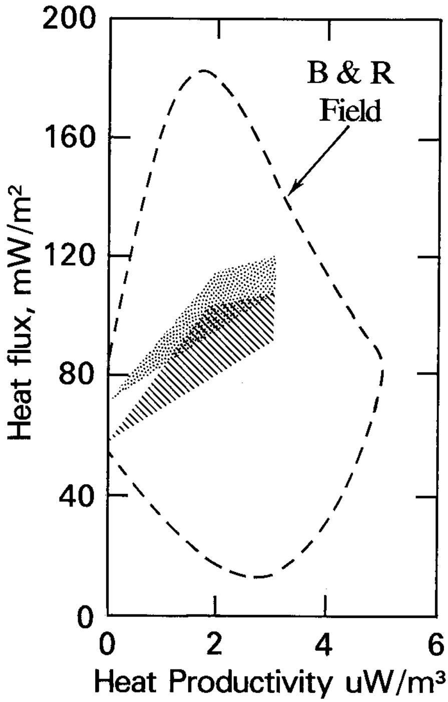

Fig. 1. Heat flow in the Basin and Range Province, based on Lachenbruch and Sass (1977). The inferred subcrustal flux for a 10-km layer of heat-producing crust is between 60 and 80 mW/m^2. Note that the lower part of the datafield for B&R is occupied mainly by the Eureka low (see text). The patterned fields define the heat productivity and maximum surface flux for the two groups of model runs having maximum subcrustal flux of 60 and 75 mW/m^2.

meter, 1 uW/m^3 = 2.4 × 10^{-7} microcalorie/cm^3-sec; Lachenbruch and Sass, 1978), but most values center around 2 to 3 uW/m^3.

MODELLING

Parameters Used

The geological and geophysical information of the Nevada portion of the B&R provides the basis for my model parameters (table 1). I used an initial thickness of 60 km and a final thickness of 30 km for the crust (see below). For all but 3 of the 37 runs this crust was thinned incrementally by instantaneous deletion, at the rate of 2 km every 2 my; for the three exceptional runs the rate was doubled (app. 1). The model extensional strain rate is 1 × 10^{-15}/sec or 3 percent per my (double that for the three runs); the vertical thinning strain rate is half that value.

TABLE 1

Values of parameters for the model (MODEL), for the Basin and Range Province (B&R), and for the Lachlan Belt (LB)

	MODEL	B&R	LB
Thermal conductivity	2.0 W/m/K		
Heat capacity	900 J/K/kg		
Rock specific gravity	2780 kg/m^3		
Crustal thickness, km			
Initial	60	~60?	
Final/present	30	30-35	35-50
Depth to mid-crustal discontinuity, km	22, 26, or 32	15-25	about 20-25
Duration of extension, my	30	>20	
Extensional Strain rate	1 x 10^{-15}/sec (3%/my)	~3-10%/my	
Heat productivity, *A*, uW/m^3	2 or 3	<3, mostly ~2	~3
Productivity/depth relations	linearly decreasing to 0 at, or constant to, 20/30 km		
Subcrustal flux, mW/m^2			
Initial	30		
Maximum	60 or 75	60-80	
Final	As above, or reduced to 40 or 45		
Surface heat flow at maximum flux	80 to 165 mW/m^2	about 90 mW/m^2; Battle Mtn high, 120-160 mW/m^2	
Time interval for adjusting thermal profile	2 my		
Final monitor depth	30 km unless otherwise stated		

Note: For model parameters, see also Zen (1988a). Basin and Range Province (B&R) tectonic data summarized from Catchings (1992), Wernicke (1992) and references therein; thermal data summarized from Lachenbruch and Sass (1977, 1978). Lachlan Belt (LB) data from Scheibner and others, (1991); Sawka and Chappell (1986).

Three depths of crustal deletion, at 20 to 22 km, 24 to 26 km, and 30 to 32 km (using 2 km thick model cells), are chosen to simulate the range of observed depth of the horizontal reflectors in the B&R; these will be referred to as the 22, 26, and 32 km depths. For one series of runs, every deletion was accompanied by a 2-km rise of the thermal interface ("thermal Moho"). Because the model is one-dimensional, only thinning can be sensed, and "deletion" could correspond to different modes of thinning and extension in the real crust, where the process is doubtless vastly more complex, where lateral transport of material and energy could happen, and where thinning could occur at different crustal levels either concurrently or sequentially. The real crust of the B&R must have thinned throughout its thickness, because the entire crust had been extended (see app. 2). I have not explored the thermal consequences of any distributed thinning.

All energy transport was assumed to be by conduction. This is reasonable because radiation is insignificant within a sialic crust and energy transport by intruding mafic magma belongs to a different model. Quantitatively significant energy transport by volatile flow *to* the site of anatexis requires an enormous amount of *hot* volatile material (Zen, 1992) and is implausible.

The entire crust is assigned a single value of thermal diffusivity (see table 1). The subcrustal heat flux is initially 30 mW/m^2 but increases with every deletion to reach a final value of either 60 or 75 mW/m^2, depending on the model, as a consequence of underplating by hot asthenospheric material in the subtended area. The crustal heat productivity, A, is either 2 or 3 uW/m^3, and the heat-producing layer extends from the surface ($Z = 0$) to a level Z' at either 20 or 30 km. The value of A either is constant to Z' or decreases linearly from the assigned value at the surface to zero at Z'. These values and thermal trajectories are compatible with values and model trajectories of Lachenbruch and Sass (1978) but extend to greater depths so as to allow for mid-crustal anatexis if fertile source material is there (see app. 3).

Of the eight initial geotherms constructed out of the triple choices in heat productivity, depth to Z', and linear versus constant relation of A and Z, three, all having constant heat productivity, are rejected because they predict *steady-state* generation of magma within the upper 30 km of the crust. The principal model parameters are listed in table 1; procedural details are given in app. 1.

Melting Properties and Temperature Ranges

The experimental data of Wyllie (1977) indicate that for starting material appropriate for strongly peraluminous 2-mica granites, the water-saturated solidus at pressures greater than ~3 kb reaches as low as 650°C, and this could be further reduced by the halogens (for review, see Zen, 1988b). If the initiation of anatexis is induced by dehydration, one might expect the first smidgeon of melt to be water-saturated, but this situation could rapidly change. I used a value of 700°C for the solidus; the small pressure dependence of the solidus above 2 to 3 kb is ignored.

I used the stepwise melting model (Zen, 1988a). Fusion occurs at 40°C intervals and is apportioned as follows: 700°C, 15 percent; 740°C, 20 percent; 780°C, 15 percent; 820°C, 10 percent; 860°C and 900°C, 5 percent each. This scheme allots most of the melting to a temperature interval of about 120°C and is intended to imitate the initial breakdown of white mica followed by a higher-temperature breakdown of more stable hydrous phases such as biotite (see Vielzeuf and Holloway, 1988; Patiño-Douce and Johnston, 1991). The parametric heat of fusion, h_f, which is the ratio of the heat of fusion to the heat capacity ($\Delta H_f/C_p$; Zen, 1988a), is 300°C: every percent of melting is energetically equivalent to lowering the temperature by 3°C. This equivalence is the basis for manipulating the temperature record to deduce the amount of melting during a run. The volume of melt varies approximately inversely with h_f.

Results of Modelling

Tables 2 to 6 summarize the results of thermal modelling. The volume of melt sensitively depends on the deletion depth (tables 2-4), but because only the melt formed above the zone of deletion is counted, the results are conservative estimates. Some trends may be noted: (1) Without increased subcrustal flux, extension causes negligible melting (table 2). (2) Paired runs (for example, tables 2 and 3, S1A/J14B; S5A/D31A; Fe15A/Fe11A) show the dependence of the result on the thickness of the heat-producing layer. (3) Paired runs (for example, tables 2 and 3, S1A/S5A; J14B/D31A; Fe15B/Fe15A; Ma3A/Fe11A) show the effect of the value of the heat-productivity. (4) A rising thermal interface with deletion results in increased melt production in all but one case (table 4, J20A/Fe3A). (5) Post-extensional thermal shutdown has negligible effect, because most melting occurred during the extension phase, yet the effect of decreased subcrustal flux is felt in the zone above deletion only many million years later (table 5). (6) Paired runs (for example, tables 2 and 3, Ja29A/J14B; Ja27A/Ja4A; J20A/J17A; Fe1B/Ma3A; Fe1A/Ja4C; Fe3A/Fe12A) show that the value of the maximum subcrustal flux, 60 versus 75 mW/m^2, has greater effect if the thermal interface rises with deletion. (7) Constant heat productivity with depth leads to significantly more melt than linearly decreasing productivity (table 5). (8) Less melt is produced at the end of deletion for faster deletion rate (table 6, part A, second entry of every pair) because the time lapse is shorter (15 my); however, *for equal time intervals* faster deletion could result in faster melt production.

Thermal, tectonic, and melting parameters that seem geologically realistic and that approximate those observed or inferred for the Basin and Range province can lead to anatexis of fertile crustal material on a regional scale and in large volumes at pressures as low as 4 kb. Deeper deletion produces more melt, but shallow deletion can result in melting at pressures where andalusite is stable. Because the melt volumes recorded here (1) ignore melts formed below the deletion zone, (2) mostly correspond to a linearly decreasing heat productivity with depth, and (3) have a relatively high solidus temperature, the small volume of melt at shallow depth of deletion is exaggerated. Heating by crustal thinning typically produces thermal responses more rapidly (10-15 my) than by crustal thickening (20-40 my).

TABLE 2

Run results using linearly decreasing heat productivity, A, from the specified value (in uW/m³) at the surface to 0 at depth Z′ (in kilometers). Fifteen deletions at specified depth, at 2 km/2 my. The basal flux, in mW/m², increases with every deletion either by 3 to 75 or by 2 to 60, without shutdown after deletion stopped at 30 my. Monitor depths constant at specified values

Run	A uW	Z′	Del at	Max basal flux	Max Q_f mW	Melt vol km^3/km^2 30	48 my	Min depth with fusion 30	48 my	Monitor depth km	Age of melt, my first	last	Max T @ 10 km
Fe25B	2	30	22	30	60	0	0	--	--	60	--	--	361
Fe25A	2	30	32	30	60	2.0	2.0	24	24	60	14	32	321
J14A	2	30	22	30	60	0	0	--	--	100	--	--	362
J9B	2	30	32	30	60	1.8	1.9	24	24	100	14	36	326
Ja29A	2	30	22	60	90	0.3	0.3	18	18	60	28	30	398
Ja27A	2	30	26	60	90	1.4	2.2	20	18	60	22	44	388
J20A	2	30	32	60	90	3.8	5.3	22	20	60	12	>50	372
S1A	2	20	22	75	95	0	0.3	--	18	60	32	44	381
J14B	2	30	22	75	105	0.5	1.3	16	16	60	26	48	428
Ja4A	2	30	26	75	105	2.1	3.4	18	16	60	20	>50	418
J17A	2	30	32	75	105	4.9	6.8	20	18	60	12	>50	401
S5A	3	20	22	75	105	0.2	0.6	18	18	60	30	>50	410
D31A	3	30	22	75	120	1.5	2.5	16	14	60	20	>50	477

TABLE 3

Run results wherein the model parameters are same as in table 2, except that the monitor depth rises by 2 km with every deletion, from an initial value of 60 km to a final value of 30 km. For the last group of three entries, the deletion rate was 2 km/my and deletion ended at 15 my

Run	A uW	Z′	Del at	Max basal flux	Max Q_f mW	Melt vol km^3/km^2 30	48 my	Min depth with fusion @ 30	48 my	Age of melt, my first	last	Max T @ 10 km
Fe15B	2	20	22	75	95	0.4	1.3	18	16	28	48	418
Ma1A	2	20	26	75	95	1.6	3.3	20	20	24	48	403
Ma1B	2	20	32	75	95	3.5	6.6	22	20	18	>50	380
Fe1B	2	30	22	60	90	0.5	0.7	18	18	26	34	405
Fe1A	2	30	26	60	90	1.6	2.3	18	18	20	>50	393
Fe3A	2	30	32	60	90	3.4	5.4	22	20	12	>50	372
Ma3A	2	30	22	75	105	1.3	2.5	18	16	24	>50	463
Ja4C	2	30	26	75	105	2.8	4.7	18	16	18	48	447
Fe12A	2	30	32	75	105	5.0	8.1	20	16	12	>50	426
Fe15A	3	20	22	75	105	0.9	1.6	16	16	26	>50	446
Fe11A	3	30	22	75	120	2.6	3.6	14	14	20	40	512
D1793A	2	30	22	75	105	0.9	2.0	18	16	13	>35	461
D1493A	2	30	26	75	105	2.1	4.2	20	18	10	>35	444
D2093A	2	30	32	75	105	3.5	7.5	24	18	6	>35	416

TABLE 4

Run results wherein the basal flux, in mW/m², increases with deletions as in table 2, then decreases after deletion stopped, either by steps of 3 to final value of 45, or by steps of 2 to final value of 40. The heat productivity, A, decreases linearly from 2 uW/m³ at the surface to 0 at 30 km except for run pair D31A/D31B, for which A is 3 uW/m³. Monitor depth held constant at 60 km. Other model parameters same as in table 2. Results in italics are from table 2

Run	Del at	Max basal flux	Max Q_f mW	Melt vol @ 30 km^3/km^2	Melt vol 48 my km^3/km^2	Min depth with fusion @ 30	Min depth with fusion 48 my	Age of melt, my first	Age of melt, my last	Max T @ 10 km
Ja29B	22	60	90	0.3	0.3	18	18	28	30	398
Ja29A				*0.3*	*0.3*	*18*	*18*	*28*	*30*	*398*
Ja29C	26	60	90	1.4	2.2	20	18	22	46	385
Ja27A				*1.4*	*2.2*	*20*	*18*	*22*	*44*	*388*
J24A	32	60	90	3.8	5.2	22	20	12	50	370
J20A				*3.8*	*5.3*	*22*	*20*	*12*	*>50*	*372*
A7A	22	75	105	0.5	1.2	16	16	26	50	424
J14B				*0.5*	*1.3*	*16*	*16*	*26*	*48*	*428*
Ja4B	26	75	105	2.1	3.2	18	18	20	50	414
Ja4A				*2.1*	*3.4*	*18*	*16*	*20*	*48*	*428*
D29A	32	75	105	4.9	6.6	20	18	12	>50	397
J17A				*4.9*	*6.8*	*20*	*18*	*12*	*>50*	*401*
D31B	22	75	120	1.5	2.3	16	14	20	>50	473
D31A				*1.5*	*2.5*	*16*	*14*	*20*	*>50*	*477*

TABLE 5

Effect of constant (C) versus linearly decreasing (L) heat productivity on melt production. The monitor depth rises from 60 to 30 km with deletions. Heat productivity, A, is 2 uW/m³ and extends to 30 km. See caption for table 2 for other conditions

Run	Del at	Max basal flux	Max Q_f mW	Melt vol @ 30 km^3/km^2	Melt vol 48 my km^3/km^2	Min depth with fusion 30	Min depth with fusion 48 my	Age of melt, my first	Age of melt, my last	Max T @ 10 km
Fe15B(L)	22	75	95	0.4	1.3	18	16	28	48	418
Ma3B(C)	22	75	115	1.8	2.9	16	14	22	>50	498
Ma1A(L)	26	75	95	1.6	3.3	20	20	24	48	403
Ma5A(C)	26	75	115	3.7	5.4	18	16	16	46	482
Ma1B(L)	32	75	95	3.5	6.6	22	20	18	>50	380
Ma12A(C)	32	75	115	5.7	8.9	20	18	8	>50	461

TABLE 6

Relation between deletion rate and melt production. All variables for paired runs are the same except for the deletion rate: 2 km/2 my for the first entry and 2 km/my for the second entry of every pair. Heat productivity, A, 2 uW/m³; thickness of productive layer, 30 km; maximum subcrustal flux, 75 mW/m²; maximum surface flux, 105 mW/m²

A. Run data

Run	Deletion depth	Volume of melt, km^3/km^2 @ end of deletion	18 my later	@ 30 my	Minimum depth of melt, km @ end of deletion	18 my later	Age of first melt, my
Ma3A	22	1.3	2.5	1.3	18	16	24
D1793A	22	0.9	2.0	1.9	18	16	13
Ja4C	26	2.8	4.1	2.8	18	16	18
D1493A	26	2.1	4.2	4.0	20	18	10
Fe12A	32	5.0	8.1	5.0	20	16	12
D2093A	32	3.5	7.5	6.8	24	18	6

B. Rate of melt production

Run	Volume of melt, km^3/km^2, end of deletion	Volume per my	Volume of melt, km^3/km^2 next 18 my	Volume per my	Overall volume per my
Ma3A	1.3	0.046	1.2	0.063	0.052
D1793A	0.9	0.059	1.1	0.060	0.060
Ja4C	2.8	0.095	1.9	0.103	0.098
D1493A	2.1	0.137	2.1	0.116	0.126
Fe12A	5.0	0.164	3.1	0.174	0.168
D2093A	3.5	0.236	4.0	0.217	0.225

Whether the melt will mobilize to form plutons depends in part on the ratio of melt to residual crystals. If the critical fraction of melt needed to mobilize a siliceous magma is around 50 percent (corresponding to a model melting interval of about 100°C), the volume of mobilized magma (melt + restite) could be much larger. In real situations, lateral pooling of magma should thicken the plutons; however, magma segregation and ascent cannot be studied using 1-dimensional modelling.

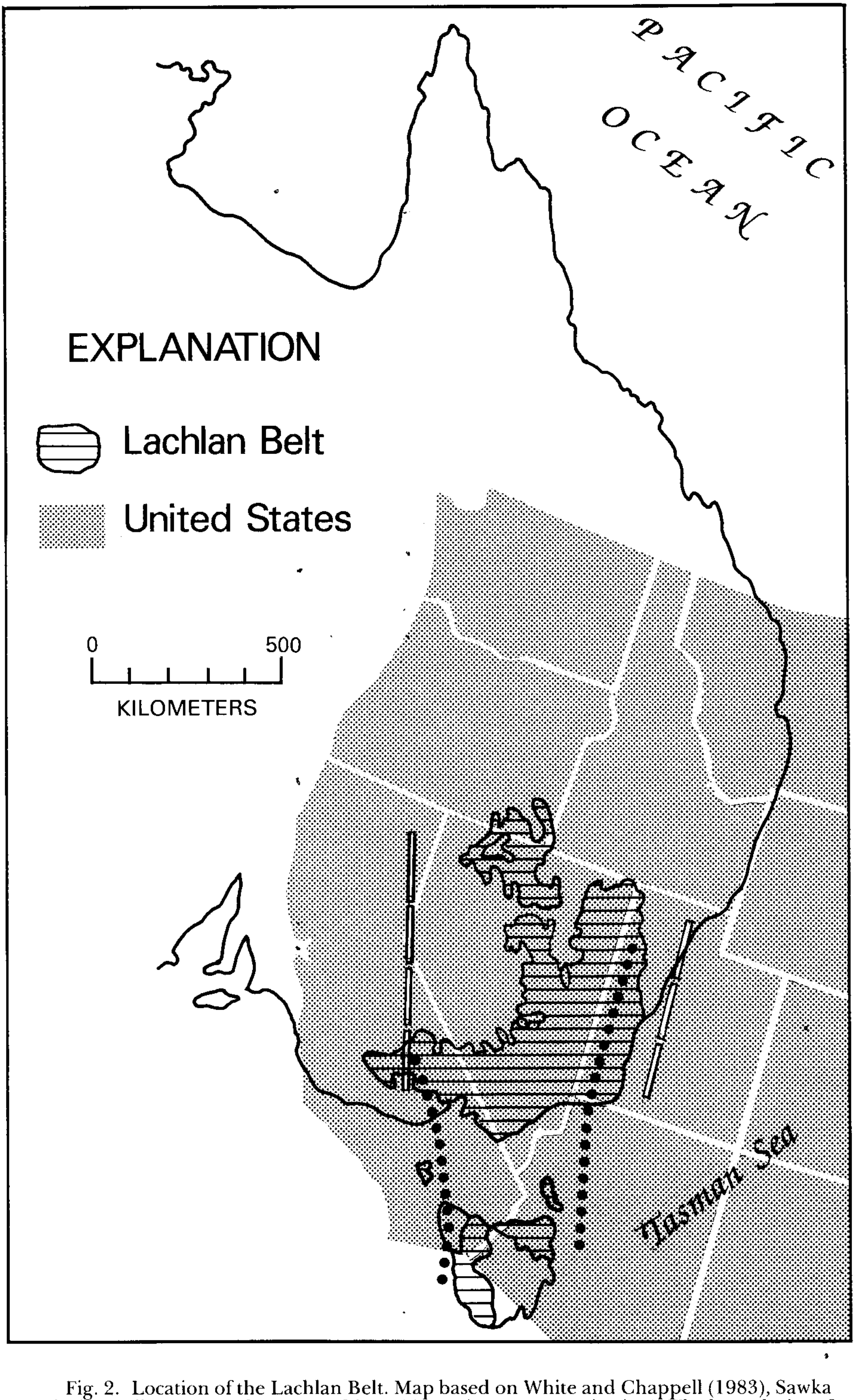

Fig. 2. Location of the Lachlan Belt. Map based on White and Chappell (1983), Sawka and Chappell (1986), and A. J. R. White, 1993 (written communication). The boundaries of the western United States are superimposed. Dotted lines, the I-S (east) and S-I (west) lines; dashed lines, the Wasatch Front and the Sierra Front.

APPLICATION TO THE LACHLAN BELT

Batholiths of the Lachlan Belt

The Lachlan Belt (LB) in New South Wales, Victoria, and Tasmania contains a complex of granitic batholiths in an area about 1100 by 700 km oriented generally north-south (fig. 2). Plutonic rocks occupy as much as 20 percent of the present land surface (Chappell, White, and Williams, 1991) and define two magmatic provinces (White and others, 1976; Chappell and others, 1991). The eastern province contains "I-type" metaluminous to slightly peraluminous, commonly hornblende-biotite bearing granites, granodiorites, tonalites, and rare gabbros ("I" for "igneous source" or "infracrustal source"; Chappell and White, 1974; Chappell, 1984). The western province contains, in addition, a large proportion of strongly peraluminous, "S-type" granite, granodiorite, and rare tonalite ("S" for "sedimentary source" or "supracrustal source"; same references), for which the source rocks must have included much undepleted or fertile sedimentary material (White and Chappell, 1988). A nearly straight line, called the I-S line, separates these two provinces at the present land surface (fig. 2).

The LB plutons were emplaced within a brief timespan of a few tens of million years at around 400 Ma or late Silurian to early Devonian (Chappell and White, 1992; Chappell, White, and Williams, 1991; D. R. Gray, 1988; C. M. Gray, 1990), with some indication that the centers of intrusion migrated west to east (Collins, 1994). The plutonic mineral assemblages indicate no major pressure difference across the width and length of the LB, with the possible exception of the tiny Three Rock pluton that may have magmatic epidote (Wyborn, 1977; pluton #408 in Chappell and others, 1991). Andalusite and sillimanite are part of the igneous and aureole assemblages where the aluminum silicate minerals occur; kyanite has not been reported. The emplacement pressure of the Tara pluton is 2.7 ± 1 kb (Miller and others, 1988; data reinterpreted using Schmidt, 1992). The Cooma complex, considered an example of *in situ* anatexis (White and Chappell, 1977), contains the assemblage sillimanite–andalusite–cordierite–biotite both in the wide "regional" aureole and in the plutonic rock, indicating a pressure of anatexis of ≤ 4 kb (see also Joplin, 1942; Flood and Vernon, 1978; Ellis and Obata, 1992). Rare almandine-rich garnet in S-type plutonic and volcanic rocks (Clemens and Wall, 1984), even if magmatic rather than xenocrystic, does not require high pressures. The wide preservation of contemporaneous and cogenetic volcanic rocks in the same structural blocks (Wyborn, Chappell, and Johnston, 1981; Wyborn, White, and Chappell, 1991; Wyborn and Chappell, 1986) and the sub-greenschist facies regional metamorphism of much of the country rock away from igneous contacts further support the inference of shallow emplacement.

Many S-type granites have major, minor, trace, rare earth-element, and stable (mainly ^{18}O) and radiogenic (mainly ^{87}Sr) isotopic patterns indicating fertile, first-generation sedimentary source rocks little modified by mafic igneous material (White and Chappell, 1988). The chemistry of the Cooma Granodiorite closely matches that of the surrounding Ordovician turbiditic marine psammite and pelite (Munksgaard, 1988; Gray, 1990); similar fertile marine sedimentary rocks unaffected by prior depletion are needed for the other S-type plutonic rocks as well. Thus, the S-type granitic rocks provide particularly useful petrogenetic constraints.

These attributes of the LB granitic rocks—their uniform, regional extent and shallow level of emplacement, the fertile crustal source rocks, the lack of subsequent major deformation or denudation (preservation of consanguineous volcanic rocks), and the environment of intrusion into regionally extensive marine turbidites, in addition to the huge thermal budget required for magma genesis—all make the origin of the LB magmas an enigma. The host Ordovician marine turbidites are typically several kilometers thick (Fergusson and Coney, 1992; Glen, 1992; Coney and others, 1990) and have been interpreted to imply deposition on a thin sialic crust (Coney, 1992); yet by Silurian time, somehow, massive amounts of fertile sedimentary source rocks were extensively being partially melted in the middle to lower portions of this initially thin crust. I will explore the thermal consequences of an assumption that this source material was tectonically intercalated into the lower half of a crust thickened, then thinned again, between the times of turbidite deposition and magma genesis.

Thermal Regimes for Crustal Magma Genesis

Before examining the possible use of my model results to the LB, a summary of the major thermal regimes that could lead to regional crustal anatexis may help to set the stage.

1. *Anatexis during crustal thickening.*—The source rock is pushed down to depths where heating by thermal relaxation causes melting. This mechanism (England and Thompson, 1984; DeYoreo, Lux, and Guidotti, 1989; Patiño-Douce, Humphreys, and Johnston, 1990; Zen, 1988a) can be expected to result in plutons recording different, mostly medium to high, pressures of anatexis, rather than a 2-dimensional field of nearly isobaric and low-pressure melting. Extensive melting should happen several tens of millions of years after compression (Zen, 1988a), and the region should show evidence of deep denudation.

2. *Thrusting hot rock over colder fertile rock.*—This mechanism could result in anatexis in fertile rocks adjacent to the thrust surface (LeFort, 1981) where the transient temperature will be the highest. The energy available for melting is limited by the temperature of the hot rock (see discussion of h_f above), and the maximum temperature of the hot overthrust rock before its fluxing by volatiles from below (France-Lanord and LeFort, 1988) is constrained by its own solidus and by the energy needed for the dehydration reactions. Thus, the mechanism should generate melts not much beyond a minimum-melt composition and be formed *in situ* or, if intruded upward, into rocks of high metamorphic grade.

3. Large-scale intrusion of basaltic magma into a fertile source terrane.—This mechanism could cause crustal anatexis (Lachenbruch and Sass, 1978; Huppert and Sparks, 1988) and is consistent with an extensional regime, but its application in a given situation requires evidence either for intimate commingling of magmas or for the production of magma of hybrid chemical character.

4. Crustal heating by massive loss of a compressionally-thickened lithosphere, through gravitational instability, and its replacement with hot asthenosphere (Collins, 1994; Loosveld and Etheridge, 1990; Gray and Cull, 1992).—This process can produce large volumes of magma as well as low-pressure, high-temperature regional metamorphism. The cycle of compression, loss of lithosphere, heating, and magma genesis, however, must be completed within a timespan consistent with the geological record.

5. Heating by crustal thinning in an extensional regime, the subject of this inquiry.—In reviewing the applicability of these regimes to the LB batholith, I conclude that the crustal thickening regime is not appropriate because of the presence of cogenetic and coeval plutonic and volcanic rocks within the same tectonic blocks, the low metamorphic grade of the surrounding country rocks, the absence of high-pressure plutons, and the lack of significant pressure gradients in this large area. The regime of thrusting hot rocks over cold is ruled out by the lack of evidence of former regional presence of overlying lower-crustal rocks or inverted metamorphic zones; further, the S-type granites have magmatic, precipitated plagioclase of An content as high as 55 percent, indicating a temperature of at least 150°C above the solidus (see below). Mixing of basaltic intrusions on a large scale is ruled out at least for the S-type magmas by lack of field and chemical evidence of contamination; moreover, these S-type granites have no igneous mafic enclaves (Chappell, White, and Williams, 1991). Finally, the regime of lithospheric loss is viable only if the cycle of events can be completed within a few tens of millions of years, which may or may not be feasible (Buck and Toksöz, 1983; Platt and England, 1994; note that Loosveld and Etheridge, 1990, assumed instantaneous lithospheric dropoff).

The tectonic, plutonic, and thermal history of the LB during its early Paleozoic evolution is unusual among major orogens (Coney, 1992), and interpretation of the data in terms of tectonic events of this time period remains controversial. Nonetheless, *some* crustal extension apparently did happen between the deposition of Ordovician turbidites and the time of the S-type magmatism (Gray, 1988; Fergusson and Coney, 1992; Coney and others, 1990; Coney, 1992; especially Cas, 1983, and Powell *in* Veevers, 1984, p. 309-329, who proposed large-scale transtensive tectonics and specifically compared the relation with that of the B&R). Collins (1994) indicated a time window of about ≤30 my for the extensional basins; this span is consistent with the record of the B&R. Sandiford and Powell (1986) proposed extensional tectonics as the cause of magma generation in the LB.

Discussion of extension requires some information on the thickness of the crust before and after extension. The present thickness of LB including the mafic lower crust is about 50 km (Scheibner, Powell, and Spencer, 1991), but it may not be used to estimate the Paleozoic thickness, nor can the current crustal architecture (Finlayson, Collins, and Denham, 1980; Scheibner, Powell, and Spencer, 1991) be safely applied to its Paleozoic counterpart. Coney (1992) suggested that during deposition of the Ordovician turbidite the crust was an attenuated continental crust no more than 10 km thick because "you cannot deposit a vast 5-km-thick deep-marine turbidite fan on "normal" 35 km continental crust." However, that constraint would not apply to the later time of middle- to lower-crustal anatexis of fertile crustal rocks. If Coney is correct, the crust subsequently must have changed thickness rather quickly; if so, both thickening and thinning could have occurred, yet the Ordovician turbidite layer somehow escaped major deformation and burial during the process. An episode of extension that lasted a few tens of millions of years cannot be excluded.

Comparison of Model Melting Properties with S-type LB Granites

The temperature range experienced by the source terranes of the S-type granitic rocks of LB can be inferred on the basis of the compositions of plagioclase in these rocks. Chappell, White, and Williams (1991) described the plagioclase in these rocks as characteristically having a core of An_{50} or more, overgrown, with a sharp boundary, by plagioclase having An_{55} or less. They attributed the cores to undissolved, though not necessarily unequilibrated, "restite" crystals, and they attributed the overgrowth to direct precipitation out of the melt phase.

The plagioclase core-overgrowth boundary is petrographically distinct. Both cores and overgrowths are twinned, but the twinning is not in optical continuity, and the overgrowth has more complex twinning (A.J.R. White, 1994, written communication). The cores are angular to rounded; some show deep embayment indicative of dissolution in the melt, supporting the restite model. Based on the plagioclase phase diagram (see Bowen, 1913; Helz, 1976; Housh and Luhr, 1991; Nekvasil, 1992), I interpret the data to mean that the composition of the outermost cores records a maximum temperature range of melting of about 150° to 180°C. Even plagioclase cores as rich as An_{80} (Chappell, White, and Williams, 1991) would merely require that portions of the magma resulted from melting over an additional temperature interval of ~ 120° to 150°C and do not demand high-An plagioclase in the source rock. Because the model thermal gradient in the melting zone is typically 40° to 50°C per kilometer, a temperature range of 150°C could imply a source-rock thickness of 3 to 4 km for particular batches of magma, in agreement with Clemens' (1988) estimate for the S-type Strathbogie batholith.

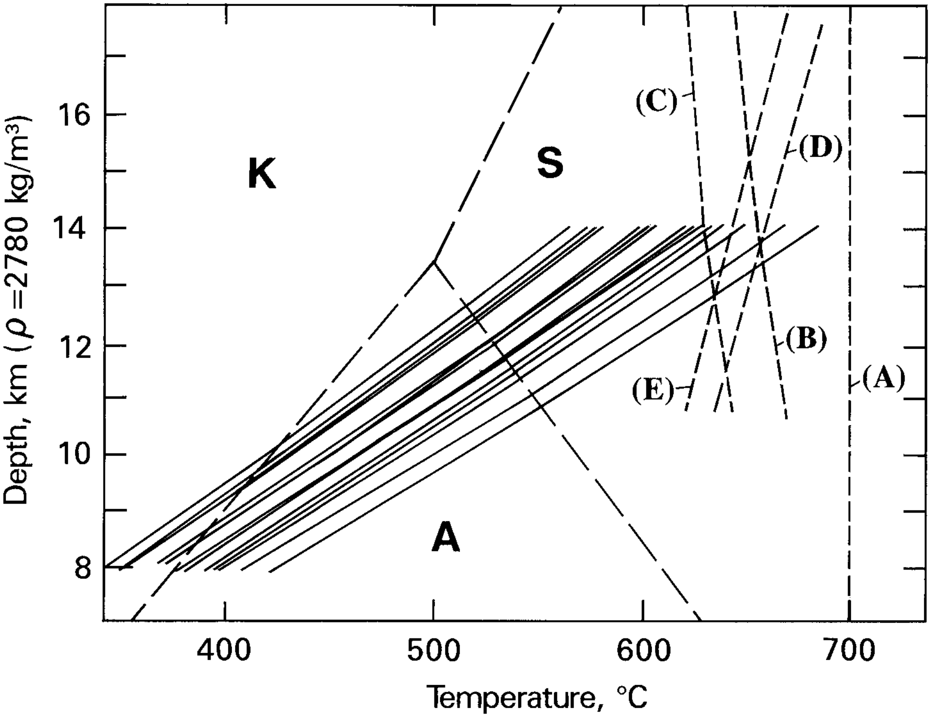

Fig. 3. PTt paths in the stationary upper crust above the level of melting and the maximum-temperature profiles showing the prograde passage from andalusite stability to sillimanite stability. Run data, left-to-right at 14-km depth: D2093A, A7A, Fe12A, J14B, Fe15A, D1493A, Ja4C, Ma12A, D1793A, Ma3A, D31B, D31A, Ma5A, Ma3B, Fe11A. The aluminum silicate phase diagram is from Holdaway (1971); a specific gravity of 2780 kg/m^3 is used to convert pressure to depth. (A) model solidus; (B) the water-saturated solidus of haplogranite (Tuttle and Bowen, 1957); (C) the water-saturated solidus of a strongly peraluminous granite (Wyllie, 1977); (D), the stability field of muscovite + quartz without plagioclase (Chatterjee and Johannes, 1974); and (E) same with plagioclase (Chatterjee and Flux, 1986).

FURTHER SPECULATIONS

Origin of Low-pressure, High-temperature Regional Metamorphism

The thermal conditions from this study provide an explanation for the origin of low-pressure, high-temperature andalusite-to-sillimanite type regional metamorphism. In the B&R, the upper crust responded to extension by listric faulting and tilting of blocks tens of kilometers wide, by formation of intermontane basins separated by linear ranges with local dipslip of several kilometer, and possibly by magma intrusion (Doughty, Price, and Parrish, 1994). Deformation was only very locally penetrative. This mode of deformation cannot be simulated by one-dimensional modelling; in the model, the crust above the deletion zone is passive.

However, in the B&R the blocks are wide relative to the downdip slip, so the model should still provide a first-order approximation of reality.

Figure 3 shows the maximum thermal profiles for 15 runs. These profiles record the maximum *synchronous* temperatures attained in the depth interval 8 to 14 km (the attainment of maximum temperature for adjacent model cells may differ by 2 my), either before the crust started to cool off, or, failing that, at the end of the runs. Within this upper crust, model PTt paths are horizontal lines whose termini define the thermal profiles, and which may traverse through the andalusite field into the sillimanite field. Because the temperature change is slow, its value at every depth stays within a few degrees of the displayed value for several million years, allowing the metamorphic assemblages to adjust to the ambient conditions.

Figure 3 also shows the "haplogranite" solidus for H_2O-saturated melt (Tuttle and Bowen, 1958), a solidus for H_2O-saturated peraluminous granite (Wyllie, 1977), and the breakdown curves for muscovite + quartz, with and without Ab-rich plagioclase (Chatterjee and Johannes, 1974; Chatterjee and Flux, 1986). Several of the model thermal profiles intersect these breakdown curves and thereby cross the second sillimanite isograd; the real rocks could be migmatitic. Thus, regional andalusite-sillimanite metamorphic facies-series can form without local magma intrusion as proposed by DeYoreo, Lux, and Guidotti (1989). Early episodes of regional low-pressure high-temperature metamorphism in regions of compressional tectonics and Barrovian regional metamorphism should alert us to look for possible palimpsest extensional events.

Did a Magma Ocean Underlie Mid-crustal Melting?

Lachenbruch (1979) called attention to the dilemma of implied wholesale melting of the lower crust if the middle crust partially melts by heat conducted from below. This dilemma cannot be dismissed by calling on non-conductive heat transport to cause melting. However, a magma ocean could be minimized by brief durations of extension, so that mid-crustal anatexis of fertile, heat-productive rocks was consummated before substantial melting of the subjacent rock, which might be either depleted and dehydrated granulite or anhydrous basalt (Lachenbruch and Sass, 1978). To make this point, figure 4A collects data on the volume of melt formed in individual runs, up to the moment when any model cell above the deletion depth reached 160°C above the solidus (see discussion on the temperature range of anatexis for the LB granites). Figure 4B, a subset of these data, includes only those runs where the crust to a depth of 30 km never exceeded 1100°C, thus permitting the lower crust to remain largely solid. Even this set of results is compatible with the volumetric calculations of Clemens (1988). Brief duration of tectonism might circumvent magma oceans beneath regions of anatexis while allowing enough magma to form to account for the plutons of LB.

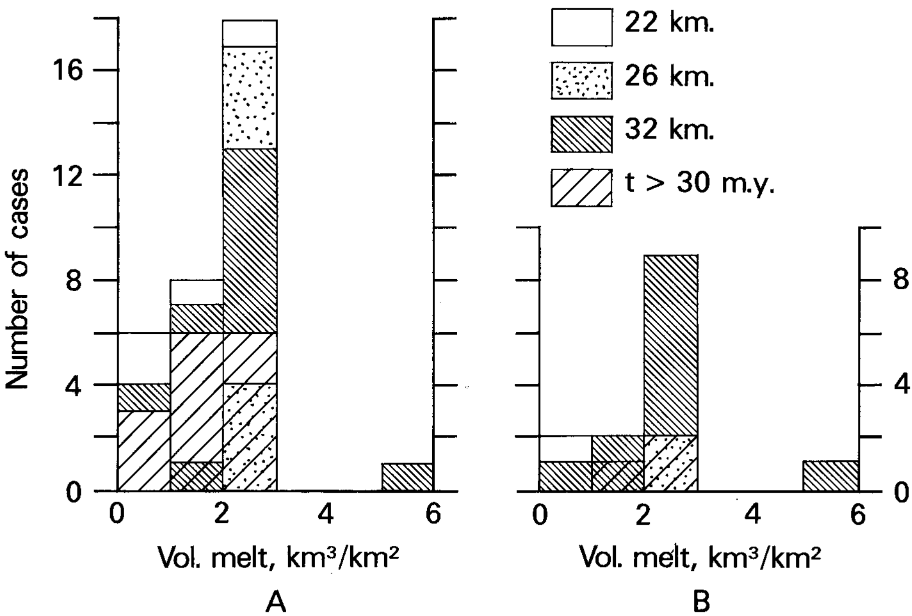

Fig. 4. Histogram of diachronous model run results of melt production for deletion rate of 2 km/2 my. (A) Melt volume, in km^3/km^2, at a point in time when at least one model cell above the deletion zone reached a temperature of 160° above the solidus. (B) A subset of (A) where the temperature in the upper 30 km of the crust was ≤ 1100°C.

Significance of the I-S Line in the LB

White and others (1976) suggested that the I-S line "probably coincides with the eastern margin of a very thick block of continental crust, possibly crystalline shield," that provided material for the S-type magmas. The results of this study suggest an alternative interpretation: east of the I-S line, the crust was unextended, and magma generation could occur only at much deeper levels, possibly beyond the depth of fertile source material for S-type magma. West of the line, mid-crustal generation of peraluminous magmas from fertile sources was possible because of enhanced heat flow, resulting in both S-type and I-type plutons. Instead of marking the eastern limit of thick crystalline crustal source material, the I-S line would mark the limit of extensional tectonics, analogous to the Wasatch Front.

If this is true, one might expect its mirror-image to the west, analogous to the Sierra Front. A.J.R. White (1993, written communication) reports such a "S-I line" in western Victoria (fig. 2), along the boundary between the Melbourne and the Stawell basement terranes (White and others, 1988; Gray, 1988). This interpretation means that the zone of extension for the LB was about 400 km wide in Victoria, nearly 3/4 the full width of the LB.

Origin of the Cooma Granodiorite in New South Wales

Genesis of the S-type Cooma Granodiorite complex has received much attention (Browne, 1914; Joplin, 1942; White and Chappell, 1977; Gray, 1990; Flood and Vernon, 1978; Munksgaard, 1988; Ellis and Obata, 1992) because (1) this apparently small body (about 4 km by 8 km) has a large prograde low-pressure high-temperature regional metamorphic aureole, best preserved on the west side; (2) the "aureole" rocks range from low greenschist facies rocks to biotite–andalusite–cordierite migmatite next to the plutonic rocks, which bears a similar igneous mineral assemblage (in contrast, most of the much-larger S-type plutons of the LB, apparently emplaced at the same depth levels, have much narrower aureoles, for example the Murrumbidgee Batholith; Joyce, 1973); and (3) the bulk chemistry and the strontium initial ratios of the Cooma Granodiorite closely resemble those of the host Ordovician marine sediments.

These relations, taken together, gave rise to the suggestion that the Cooma Granodiorite resulted from *in situ* total fusion of the sediments; but why should such a small pluton be the locus of total fusion? Four possibilities come to mind. The high-grade metamorphic rocks and the igneous rocks might have been uplifted relative to the lower grade rocks (Flood and Vernon, 1978). The Cooma body might once have been larger, its eastern part being truncated by a north-south fault (the "White Gneiss" of Browne, 1914, exposed along the Monaro Highway at Bunyan, is a pervasively sheared rock displaying prominent S-C fabric). The wide metamorphic aureole on the west side might reflect a shallow contact, consistent with the low-dipping foliation of the migmatite there. Finally, the Cooma pluton might have been the conduit for ascending magma (to an overlying volcano?). I calculated the thermal effect due to static conductive heating by a vertical pipe, with temperature fixed at 800°C at the contact by the passage of magma, and a country rock at 300°C initially and at farfield. The observed western aureole configuration can be simulated by magma passage for a few hundred thousand years; briefer if the western contact is shallow.

Because the mineral assemblage of Cooma pluton implies pressure not more than 4 kb, if formed *in situ,* the pluton requires an average vertical thermal gradient from the surface of at least 50°C per kilometer. The model runs show that such thermal gradients are not unreasonable: deletion at 20 to 22 km depth, in particular, could produce melt at a depth of only 14 km, which for bulk specific gravity of 2780 kg/m^3 would be nearly at the triple-point depth for the aluminum silicates (fig. 5). Upward magma flow would help maintain a steep gradient. One could challenge that the Cooma plutonic rocks, locally full of decimenter-sized biotite-cordierite rich enclaves (Chappell, White, and Williams, 1991), could not have moved far. However, we do not really know the physical role played by these relatively dense enclaves; for instance, if they were

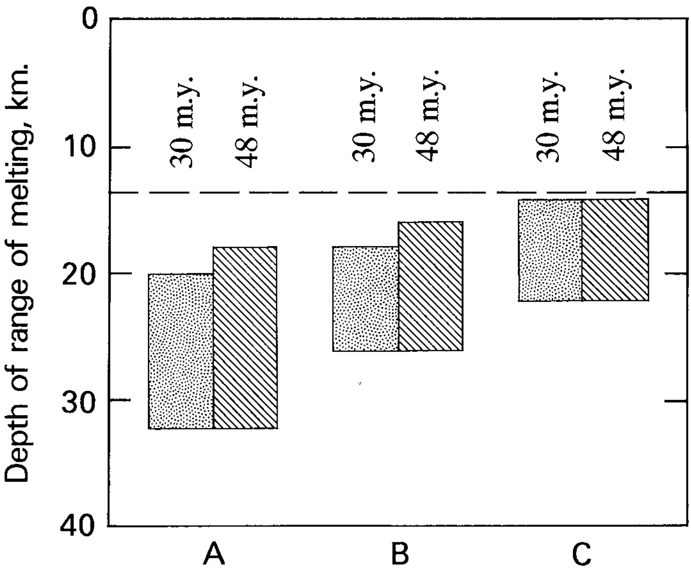

Fig. 5. Depth range of anatexis, exclusively above the deletion depth, for different model deletion depths (A, 30-32 km; B, 24-26 km; and C, 20-22 km), and for two model times (left, 30 my; right, 48 my). Horizontal dashed line, the depth of the triple point of the aluminum silicate polymorphs for rocks having a specific gravity of 2780 kg/m^3.

cumulate dregs in an upward-draining magma chamber, then their presence would not necessarily argue against magma mobility.

ACKNOWLEDGMENTS

This study grew out of a visit to the LB in 1991 as a Visiting Fellow at the Australian National University. I thank Bruce B. Chappell for arranging the visit and for introducing me to the rocks; Arthur H. Lachenbruch for instructive discussions of the thermal history of B&R; R. Brooks Hanson for checking my calculations for the Cooma complex by a 2-D computer run; Allan J.R. White, Charles V. Guidotti, David J. Ellis, and Leslie A.I. Wyborn for sharing ideas and data; and Susan W. Kieffer for field support and sharing the encounter with a yellow-bellied black snake. Charlotte M. Allen, Michael Brown, Robert Gregory, Art Lachenbruch, Philip Piccoli, Nicholas B. Woodward, and Allan White reviewed the manuscript. I am indebted to them for their constructive and thoughtful comments even though I did not always agree with them.

APPENDIX I

Details on Modelling

The steady-state continental geotherm was used as the "prescribed" geotherm to initiate a run (Haugerud, 1986). The run begins with the deletion of a 2-km thick model cell. Then, at the fixed model time for deletion (normally every 2 my), the computations are interrupted, and the current temperature profile filed. The next iteration brings this file to the screen; the temperature value for the deleted cell is replaced by that of the next lower cell, and so forth, until all the cells below the deletion depth have been replaced. This new profile is used to complete the iteration.

For a given run, the depth to the thermal interface (monitoring depth) either decreases by 2 km with every deletion or stays unchanged. For the first option, the substitution procedure described above poses no problem. For the second option, however, the computer contains no information on the temperature of the cell *below* the lowest one. I ran subsidiary steady-state thermal profiles for different basal flux values to depths included in the main runs; appropriate thermal *gradients* from these subsidiary runs are then used to estimate the temperature of the last cell.

Increase in subcrustal flux is by fixed increments, and the pre-determined maximum subcrustal flux is attained at the end of the extensional episodes. The final, maximum subcrustal flux value is either 60 or 75 mW/m^2. The corresponding increments were 2 or 3 mW/m^2, and the corresponding surface flux at the end of extension ranges from 80 to 120 mW/m^2. These values are similar to those proposed by Lachenbruch and Sass (1978).

Because only the melt formed above the zone of deletion is counted during the runs, the temperature above the deletion depth is the target of attention. If it exceeds the solidus temperature anywhere above the deletion zone, melting happens, and the amount of melt is computed (Zen, 1988a).

The temperature record of the vertical rock column, thus, may be manipulated by deletion, with cell-by-cell upward adjustment of temperature, and by melting above the zone of deletion. The two processes happen in different parts of the rock column and do not interfere with each other.

The process is iterated 15 times to the end of deletion, normally 30 my into model time. At that time, melting may have already ceased. If not, the model run is continued for another 18 my. During the post-deletion phase, again two thermal options are available: the subcrustal flux is either kept at the maximum level or is reduced stepwise for 10 iterations to attain the final values of 45 mW/m^2 and 40 mW/m^2, respectively, for the maximum flux values of 75 and 60 mW/m^2.

APPENDIX 2

Accommodation to Extension by the Upper Crust

In the model study, the upper crust remained static and maintained its thickness. In the real world, the original upper crust must extend and thin as well. If the depth to the horizontal seismic reflectors, that is, the upper crust-middle crust boundary, corresponds to the brittle-ductile transition, then this depth could be expected to migrate downward relative to some material marker when the upper crust is thinned. Thus, the upper crust, which supported extension by brittle failure, is replenished from below through a lowering of the top of the zone of detachment. This migration would entail some advective heat transport not accommodated by the conductive model.

For the Lachlan Belt, part of the extension may be accommodated by passive intrusion of batholiths. To test this idea, I made five east-west (normal to the elongate batholiths) linear traverses of the map of the LB batholiths (Chappell and others, 1991) at intervals of half-degree latitude from 34°30′S to 36°30′S. Each traverse extends from the west exposed edge of the LB to the Pacific Ocean, and the traverses have a cumulative length of 2000 km. The proportions of the land occupied by batholithic rocks (areas of volcanic rocks were ignored) were recorded. If the batholiths were passive intrusions in an extensional environment, the linear data can be interpreted as a nominal elongation factor of 1.5, to be compared with the overall elongation factor of 2 for the Basin and Range Province. Along with listric faulting, passive intrusion might be a significant contributor to upper crustal extension.

Appendix 3

Heat Productivity of Peraluminous Granites

Sawka and Chappell (1986), quoting Sass and Lachenbruch (1979), gave values of radioactive heat productivity, A, for seven LB plutons as ranging between 2 and 3 uW/m^3 (the values include the Mesozoic monzonitic Mount Dromedary pluton; see Chappell, White, and Williams, 1991). The chemical data for S-type granites (Chappell, White, and Williams, 1991) yielded, using the conversion ratios of Wetherill (1966), an average value of A of 2.96 ± 0.54 (range, 2.14-4.40; n = 22; one standard deviation). For the S-type Cowra Granite (Wyborn, White, and Chappell, 1991), the value of A is 2.79 ± 0.13, range 2.52 to 3.01 (n = 11). Both values are consistent with an A value of 2.76 for the "average S-type granite," based on 609 analyses (Chappell, White, and Williams, 1991). For the same 22 samples, the contribution from U and Th alone is 2.62 ± 0.51, range 1.83 to 3.96.

The heat productivity of crustal anatectic granite should provide an upper estimate of that of the source material (Zen, 1992). The argument for strong partition of K into the melt is clear, but that for Th and U is less so and anecdotal information must do. For the Cooma Granodiorite, the major and trace element data for the igneous rock are nearly identical to those for the surrounding Ordovician marine sedimentary rocks that have been suggested to be the source (Munksgaard, 1988); their U and Th contents are nearly indistinguishable. The contribution of U and Th to heat productivity of the Cooma Granodiorite is the same as that for the average S-type granite. If the Cooma Granodiorite were indeed derived from a source chemically like the Ordovician sediments, all the undissolved material must have been virtually completely entrained as restite. Because the Th, U contribution to heat productivity of the S-type granite is about 60 percent more than the "average crust" or the old rocks of the Canadian Shield (Zen, 1992), these elements presumably did not partition into that part of the restite not entrained into the magma. If the source material for the S-type granites of LB was not fertile sedimentary rocks but old crystalline basement (White, Williams, and Chappell, 1976), the need for concentration of the heat-producing elements into the magma would be even stronger.

References

Blackwell, D. D., and Steele, J. L., editors, 1991, Geothermal map of North America: Geological Society of America, Map CSM-006, scale 1:5,000,000, 4 sheets.

Bowen, N. L., 1913, Melting phenomenon of plagioclase feldspar: American Journal of Science, 4th series, v. 35, p. 577–599.

Browne, W. R., 1914, The geology of the Cooma District, N.S.W., Part I: Royal Society of New South Wales Journal, v. 48, p. 172–222.

Buck, W. R., and Toksöz, M. N., 1983, Thermal effects of continental collisions: thickening a variable viscosity lithosphere: Tectonophysics, v. 100, p. 53–69.

Cas, Ray, 1983, A review of the palaeogeographic and tectonic development of the Palaeozoic Lachlan Fold Belt of southeastern Australia: Geological Society of Australia, Special Publication 10, 104 p.

Catchings, R. D., 1992, A relation among geology, tectonics, and velocity structure, western to central Nevada Basin and Range: Geological Society of America Bulletin, v. 104, p. 1178–1192.

Catchings, R. D., and Mooney, W. D., 1991, Basin and Range crustal and upper mantle structure, northwest to central Nevada: Journal of Geophysical Research, v. 96, no. B4, p. 6247–6267.

Chappell, B. W., 1984, Source rocks of I- and S-type granites in the Lachlan Fold Belt, southeastern Australia: Royal Society of London, Philosophical Transactions, v. A310, p. 693–707.

Chappell, B. W., English, P. M., King, P. L., White, A. J. R., and Wyborn, D., 1991, Granites and related rocks of the Lachlan Fold Belt: Australia Bureau of Mineral Resources, Geology and Geophysics, 1 sheet, scale 1:1,250,000.

Chappell, B. W., and White, A. J. R., 1974, Two contrasting granite types: Pacific Geology, v. 8, p. 173–174.
———— 1992, I- and S-type granites in the Lachlan Fold Belt: Royal Society of Edinburgh, Transactions, Earth Sciences, v. 83, p. 1–26 (also available as Geological Society of America Special Paper 272).
Chappell, B. W., White, A. J. R., and Williams, I. S., 1991, Second Hutton Symposium on granites and related rocks, Canberra, 1991, Excursion Guide, A transverse section through granites of the Lachlan Fold Belt: Australia Bureau of Mineral Resources, Geology and Geophysics, Record 1991/22, 125 p.
Chatterjee, N. D., and Flux, S., 1986, Thermodynamic mixing properties of muscovite-paragonite crystalline solutions at high temperatures and pressures, and their geological applications: Journal of Petrology, v. 27, p. 677–693.
Chatterjee, N. D., and Johannes, Wilhelm, 1974, Thermal stability and standard thermodynamic properties of synthetic $2M_1$-muscovite, $KAl_2[AlSi_3O_{10}(OH)_2]$: Contributions to Mineralogy and Petrology, v. 48, p. 89–114.
Clemens, J. D., 1988, Volume and composition relationships between granites and their lower crustal source regions: an example from central Victoria, Australia: Australian Journal of Earth Sciences, v. 35, p. 445–449.
Clemens, J. D., and Wall, V. J., 1984, Origin and evolution of a peraluminous silicic ignimbrite suite: the Violet Town Volcanics: Contributions to Mineralogy and Petrology, v. 88, p. 354–371.
Collins, W. J., 1994, Upper- and middle-crustal response to delamination: an example from the Lachlan Fold Belt, eastern Australia: Geology, v. 22, p. 143–146.
Coney, P. J., 1992, The Lachlan belt of eastern Australia and circum-Pacific tectonic evolution: Tectonophysics, v. 214, p. 1–25.
Coney, P. J., Edwards, Alaster, Hine, Richard, Morrison, Fiona, and Windrim, Donal, 1990, The regional tectonics of the Tasman orogenic system, eastern Australia: Journal of Structural Geology, v. 12, p. 519–543.
DeYoreo, J. J., Lux, D. R., and Guidotti, C. V., 1989, The role of crustal anatexis and magma migration in the thermal evolution of regions of thickened continental crust, *in* Daly, J. S., Cliff, R. A., and Yardley, B. W. D., editors, Evolution of metamorphic belts: Geological Society of London Special Publication 43, p. 187–202.
Doughty, P. T., Price, R. A., and Parrish, R. R., 1994, Accommodation of crustal extension by regional strain and magma intrusion within the Priest River Complex, U.S.A.: Geological Society of America, Abstracts with Programs, v. 26, p. 49.
Eaton, G. P., 1980, Geophysical and geological characteristics of the crust of the Basin and Range Province: National Research Council, Continental Tectonics, p. 96–113.
Ellis, D. J., and Obata, M., 1992, Migmatite and melt segregation at Cooma, New South Wales: Royal Society of Edinburgh, Transactions, Earth Sciences, v. 83, p. 95–106 (also available as Geological Society of America Special Paper 272).
England, P. C., and Thompson, A. B., 1984, Pressure-temperature-time paths of regional metamorphism. Part I, heat transfer during the evolution of regions of thickened crust: Journal of Petrology, v. 25, p. 894–928.
Fergusson, C. L., and Coney, P. J., 1992, Convergence and intraplate deformation in the Lachlan Fold Belt of southeastern Australia: Tectonophysics, v. 214, p. 417–439.
Finlayson, D. M., Collins, C. D. N., and Denham, D., 1980, Crustal structure under the Lachlan Fold Belt, southeastern Australia: Physics of the Earth and Planetary Interiors, v. 21, p. 321–342.
Flood, R. H., and Vernon, R. H., 1978, The Cooma Granodiorite, Australia: an example of in situ crustal anatexis?: Geology, v. 6, p. 81–84.
France-Lanord, Christian, and LeFort, Patrick, 1988, Crustal melting and granite genesis during the Himalayan collision orogenesis: Royal Society of Edinburgh, Transactions, Earth Sciences, v. 79, p. 183–195.
Glen, R. A., 1992, Thrust, extensional and strike-slip tectonics in an evolving Paleozoic orogen—a structural synthesis of the Lachlan Orogen of southeastern Australia: Tectonophysics, v. 214, p. 341–380.
Gray, C. M., 1990, A strontium isotopic traverse across the granitic rocks of southeastern Australia: petrogenetic and tectonic implications: Australian Journal of Earth Sciences, v. 37, p. 331–349.
Gray, D. R., 1988, Structure and tectonics, Chapter 1, *in* Douglas, J. G., and Ferguson, J. A., editors, Geology of Victoria: Geological Society of Australia, Victoria Division, p. 1–36.

Gray, D. R., and Cull, J. P., 1992, Thermal regimes, anatexis, and orogenesis: relations in the western Lachlan Fold Belt, southeastern Australia: Tectonophysics, v. 214, p. 441–461.

Gray, D. R., Wilson, C. J. L., and Barton, T. J., 1991, Intracrustal detachments and implications for crustal evolution within the Lachlan fold belt, southeastern Australia: Geology, v. 19, p. 574–577.

Haugerud, R. A., 1986, 1DT—an interactive, screen-oriented microcomputer program for simulation of 1-dimensional geothermal histories: U.S. Geological Survey, Open-file Report 86–511.

Helz, R. T., 1976, Phase relations of basalts in their melting ranges at P_{H2O} = 5 kb, Part II, melting compositions: Journal of Petrology v. 17, p. 139–193.

Holdaway, M. J., 1971, Stability of andalusite and the aluminum silicate phase diagram: American Journal of Science, v. 271, p. 97–131.

Housh, T. B., and Luhr, J. F., 1991, Plagioclase-melt equilibria in hydrous systems: American Mineralogist v. 76, p. 477–492.

Huppert, H. E., and Sparks, R. S. J., 1988, The generation of granitic magmas by intrusion of basalt into continental crust: Journal of Petrology, v. 29, p. 599–624.

Joplin, G. A., 1942, Petrological studies in the Ordovician of New South Wales. I. The Cooma Complex: The Linnean Society of New South Wales, Proceedings, v. 67, p. 156–196.

Joyce, A. S., 1973, Petrogenesis of the Murrumbidgee batholith, A.C.T.: Geological Society of Australia Journal v. 20, p. 179–197.

Lachenbruch, A. H., 1979, Heat flow in the Basin and Range Province and thermal effects of tectonic extension: Pure and Applied Geophysics, v. 117, p. 34–50.

Lachenbruch, A. H., and Sass, J. H., 1977, Heat flow in the United States and the thermal regime of the crust, *in* Heacock, J. H., editor, The Earth's crust, its nature and physical properties: American Geophysical Union Geophysical Monograph 20, p. 626–675.

———— 1978, Models of an extending lithosphere and heat flow in the Basin and Range province: Geological Society of America Memoir 152, p. 209–250.

LeFort, Patrick, 1981, Manaslu leucogranite: a collision signature of the Himalaya, a model for its genesis and emplacement: Journal of Geophysical Research, v. 86B, p. 10,545–10,568.

Loosveld, R. J. H., and Etheridge, M. A., 1990, A model for low-pressure facies metamorphism during crustal thickening: Journal of Metamorphic Geology, v. 8, p. 257–267.

Miller, C. M., Watson, E. B., and Harrison, T. M., 1988, Perspectives on the source, segregation, and transport of granitoid magmas: Royal Society of Edinburgh, Transactions, Earth Sciences, v. 79, p. 135–156.

Munksgaard, N. C., 1988, Source of the Cooma Granodiorite, New South Wales—a possible role of fluid-rock interaction: Australian Journal of Earth Sciences, v. 35, p. 363–377.

Nekvasil, Hanna, 1992, Feldspar crystallisation in felsic magmas: a review: Royal Society of Edinburgh, Transactions, Earth Sciences, v. 83, p. 399–407.

Patiño-Douce, A. E., Humphreys, E. D., and Johnston, A. D., 1990, Anatexis and metamorphism in tectonically thickened continental crust exemplified by the Sevier hinterland, western North America: Earth and Planetary Science Letters, v. 97, p. 290–315.

Patiño-Douce, A. E., and Johnston, A. D., 1991, Phase equilibria and melt productivity in the pelitic system: implications for the origin of peraluminous granitoids and aluminous granulites: Contributions to Mineralogy and Petrology, v. 107, p. 202–218.

Platt, J. P., and England, P. C., 1994, Convective removal of lithosphere beneath mountain belts: thermal and mechanical consequences: American Journal of Science, v. 294, p. 307–336.

Sandiford, Michael, and Powell, Roger, 1986, Deep crustal metamorphism during continental extension: modern and ancient examples: Earth and Planetary Science Letters, v. 79, p. 151–158.

Sass, J. H., and Lachenbruch, A. H., 1979, Thermal regime of the Australian continental crust, McElhinny, M. W., editor, *in* The Earth: its origin, structure and evolution: New York, Academic Press, p. 301–351.

Sawka, W. N., and Chappell, B. W., 1986, The distribution of radioactive heat production in I- and S-type granites and residual source regions: implications to high heat flow areas in the Lachlan Fold Belt, Australia: Australian Journal of Earth Sciences, v. 33, p. 107–118.

Scheibner, Erwin, Powell, C. McA., and Spencer, Ross, 1991, Global Geoscience Transect 5, Broken Hill–Sydney–Tasman Sea transect, New South Wales, eastern Australia: American Geophysical Union and the Inter-Union Commission on the Lithosphere, 29 p. + maps and sections, 2 sheets, scale 1:1,000,000.

Schmidt, M. W., 1992, Amphibole composition in tonalite as a function of pressure: an experimental calibration of the Al-in-hornblende-barometer: Contributions to Mineralogy and Petrology, v. 110, p. 304–310.

Tuttle, O. F., and Bowen, N. L., 1958, Origin of granite in the light of experimental studies in the system $NaAlSi_3O_8$-$KAlSi_3O_8$-H_2O: Geological Society of America Memoir 74, 153 p.

Veevers, J. J., editor, 1984, Phanerozoic earth history of Australia: Oxford, Clarendon Press, 418 p.

Vielzeuf, D., and Holloway, J. R., 1988, Experimental determination of the fluid-absent melting relations in the pelitic system: Contributions to Mineralogy and Petrology v. 98, p. 257–276.

Wernicke, Brian, 1992, Cenozoic extensional tectonics of the U.S. Cordillera, *in* Burchfiel, B. C., Lipman, P. W., and Zoback, M. L., editors, The Cordilleran orogen; conterminous United States: Geological Society of America, The geology of North America, v. G3, p. 553–583.

Wernicke, Brian, Axen, G. J., and Snow, J. K., 1988, Basin and Range extensional tectonics at the latitude of Las Vegas, Nevada: Geological Society of America Bulletin v. 100, p. 1738–1757.

Wetherill, G. W., 1966, Radioactive decay constants and energies: *in* Clark, S. P., Jr., editor, Handbook of Physical Constants, Geological Society of America Memoir 97, p. 513–519.

White, A. J. R., and Chappell, B. W., 1977, Ultrametamorphism and granitoid genesis: Tectonophysics, v. 43, p. 7–22.

——— 1983, Granitoid types and their distribution in the Lachlan Fold Belt, southeastern Australia: Geological Society of America Memoir 159, p. 21–34.

——— 1988, Some supracrustal (S-type) granites of the Lachlan Fold Belt: Royal Society of Edinburgh, Transactions, Earth Sciences, v. 79, p. 169–181.

White, A. J. R., Chappell, B. W., Price, R. C., Gray, C. M., Nicholls, I. A., and Day, A., 1988, Petrology of igneous rocks, Chapter 11, *in* Douglas, J. G. and Ferguson, J. A., editors, Geology of Victoria: Geological Society of Australia, Victoria Division, p. 427–439.

White, A. J. R., Williams, I. S., and Chappell, B. W., 1976, The Jindabyne thrust and its tectonic, physiographic and petrogenetic significance: Geological Society of Australia Journal, v. 23, Part 1, p. 105–112.

Winograd, I. J., and Thordarson, W., 1975, Hydrogeologic and hydrochemical framework, south-central Great Basin, Nevada-California, with special reference to the Nevada Test Site: U.S. Geological Survey Professional Paper 712-C, 126 p.

Wyborn, D., and Chappell, B. W., 1986, The petrogenetic significance of chemically related plutonic and volcanic rock units: Geological Magazine, v. 123, p. 619–628.

Wyborn, D., Chappell, B. W., and Johnston, R. M., 1981, Three S-type volcanic suites from the Lachlan Fold Belt, southeast Australia: Journal of Geophysical Research, v. 86B, p. 10,335–10,348.

Wyborn, D., White, A. J. R., and Chappell, B. W., 1991, Second Hutton Symposium on granites and related rocks, Canberra, 1991, Excursion Guide, Enclaves in the S-type Cowra Granodiorite: Australia, Bureau of Mineral Resources, Geology and Geophysics, Record 1991/24, 33 p.

Wyborn, L. A. I., ms, 1977, Aspects of the geology of the Snowy Mountains region and their implications for the tectonic evolution of the Lachlan Fold Belt: Ph.D. thesis, Australian National University.

Wyllie, P. J., 1977, Crustal anatexis: an experimental review: Tectonophysics, v. 43, p. 41–71.

Zen, E-an, 1988a, Thermal modelling of stepwise anatexis in a thrust-thickened sialic crust: Royal Society of Edinburgh, Transactions, Earth Sciences, v. 79, p. 223–235.

——— 1988b, Phase relations of peraluminous granitic rocks and their petrogenetic implications: Annual Review of Earth and Planetary Sciences, v. 16, p. 21–51.

——— 1992, Using granite to image the thermal state of the source terrane: Royal Society of Edinburgh, Transactions, Earth Sciences, v. 83, p. 107–114 (also available as Geological Society of America Special Paper 272).